

Emission of Electric Dipole Radiation in Between Parallel Mirrors

Henk F. Arnoldus,^{a,*} Zhangjin Xu,^a

^aDepartment of Physics and Astronomy, Mississippi State University, Mississippi State, USA, 39762

Abstract. An oscillating electric dipole in free space emits its energy along straight lines. When the dipole is located in between parallel mirrors, this mechanism is significantly altered. Interference between the electric field of the dipole and the reflected magnetic field by the mirrors leads to a four-vortex structure in the emission pattern. The strength of the vortices depends on the separation between the mirrors and the distance of the dipole to one of the mirrors through a universal function.

Keywords: Dipole radiation, Poynting vector, parallel mirrors.

* Correspondence Author, E-mail: hfal@msstate.edu

1 Introduction

Characteristics of emitted electromagnetic radiation by an oscillating electric dipole are not only determined by the dipole itself but also by its environment. The most celebrated phenomenon is the alteration of the energy emission rate due to the presence of an interface with a material medium. Radiation reflected back to the dipole by the interface changes the local electric field and this leads to either an enhancement or an inhibition of the energy emission rate.¹⁻⁸ A natural generalization is the situation where the emitting dipole is located in between two parallel plane interfaces,⁹ with the most interesting case being power emission in between parallel mirrors.¹⁰⁻¹³

2 Dipole in between mirrors

We consider an electric dipole, oscillating at angular frequency ω , and located in between parallel mirrors, separated by a distance L . The lower mirror is the xy plane and the z axis is perpendicular to both mirrors, with the positive end up. The dipole is located on the z axis, a distance H above the lower mirror. The dipole moment is written as $\mathbf{d} = d_0 \mathbf{u}$, with d_0 the amplitude of the oscillation and \mathbf{u} a unit vector indicating the direction of oscillation. We shall assume that the dipole oscillates under angle γ with the positive z axis, so that

$$\mathbf{u} = \mathbf{e}_z \cos \gamma + \mathbf{e}_y \sin \gamma \quad . \quad (1)$$

The setup is illustrated in Figure 1. The reflected field is identical to the field radiated by an infinite sequence of images on the z axis. They are located at

$$z_m = (m + \frac{1}{2})L + (-1)^m (H - \frac{1}{2}L) \quad , \quad (2)$$

with m any integer. The ‘image’ with $m = 0$ is the dipole itself, and we have $z_0 = H$. The dipole

moment of the m^{th} image is $\mathbf{d}_m = d_o \mathbf{u}_m$, with

$$\mathbf{u}_m = \mathbf{e}_z \cos \gamma + (-1)^m \mathbf{e}_y \sin \gamma \quad (3)$$

For m even, $\mathbf{u}_m = \mathbf{u}$, and this is the dipole moment vector of the dipole itself, as in Eq. (1). For m odd, the parallel component changes sign.

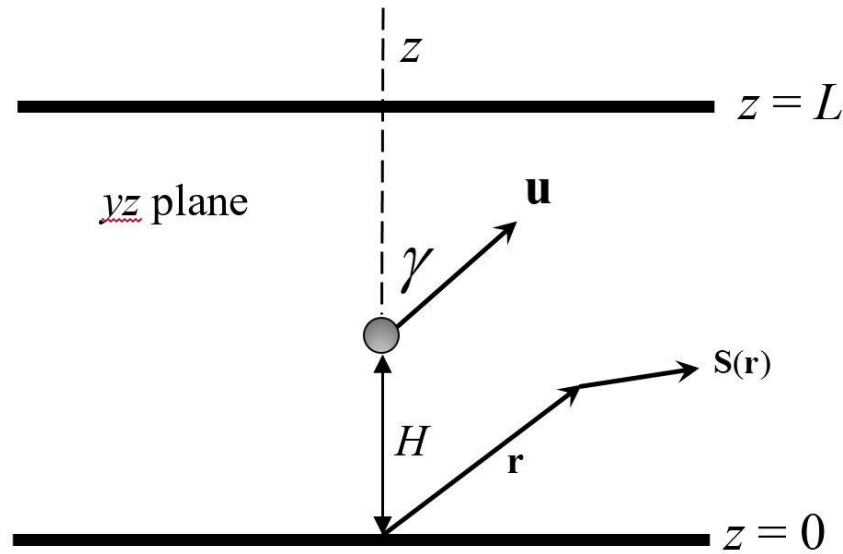


Fig. 1 The figure shows the dipole in between the mirrors.

3 Fields

Let

$$\zeta = \frac{k_o^3 d_o}{4\pi\epsilon_o} \quad (4)$$

with $k_o = \omega / c$ the wave number of the radiation. For the electric field $\mathbf{E}(\mathbf{r})$ and the magnetic field $\mathbf{B}(\mathbf{r})$ we split off a factor as

$$\mathbf{E}(\mathbf{r}) = \zeta \mathbf{e}(\mathbf{r}) \quad (5)$$

$$\mathbf{B}(\mathbf{r}) = \frac{\zeta}{c} \mathbf{b}(\mathbf{r}) \quad (6)$$

The field point \mathbf{r} with respect to the location of the m^{th} image is

$$\mathbf{r}_m = \mathbf{r} - z_m \mathbf{e}_z \quad (7)$$

The dimensionless distance between the m^{th} image and the field point is $q_m = k_o r_m$, and unit vector $\hat{\mathbf{r}}_m$ points from the m^{th} image to the field point. The complex amplitudes of the electric

and magnetic fields of the m^{th} image can then be written as

$$\mathbf{e}_m(\mathbf{r}) = \left\{ \mathbf{u}_m - (\mathbf{u}_m \cdot \hat{\mathbf{r}}_m) \hat{\mathbf{r}}_m + [\mathbf{u}_m - 3(\mathbf{u}_m \cdot \hat{\mathbf{r}}_m) \hat{\mathbf{r}}_m] \frac{i}{q_m} \left(1 + \frac{i}{q_m} \right) \right\} \frac{e^{iq_m}}{q_m} , \quad (8)$$

$$\mathbf{b}_m(\mathbf{r}) = (\hat{\mathbf{r}}_m \times \mathbf{u}_m) \left(1 + \frac{i}{q_m} \right) \frac{e^{iq_m}}{q_m} . \quad (9)$$

The total electric and magnetic fields in between the mirrors are the sums over the contributions from all images, including the dipole itself:

$$\mathbf{e}(\mathbf{r}) = \sum_{m=-\infty}^{\infty} \mathbf{e}_m(\mathbf{r}) , \quad (10)$$

$$\mathbf{b}(\mathbf{r}) = \sum_{m=-\infty}^{\infty} \mathbf{b}_m(\mathbf{r}) . \quad (11)$$

4 Poynting vector and flow lines of energy

The flow lines of electromagnetic energy are represented by the field lines of the Poynting vector.

The time-averaged Poynting vector in free space at the field point \mathbf{r} is

$$\mathbf{S}(\mathbf{r}) = \frac{1}{2\mu_0} \text{Re}[\mathbf{E}(\mathbf{r}) \times \mathbf{B}(\mathbf{r})^*] . \quad (12)$$

We set

$$\mathbf{S}(\mathbf{r}) = \frac{\zeta^2}{2\mu_0 c} \boldsymbol{\sigma}(\mathbf{r}) , \quad (13)$$

so that we have

$$\boldsymbol{\sigma}(\mathbf{r}) = \text{Re}[\mathbf{e}(\mathbf{r}) \times \mathbf{b}(\mathbf{r})^*] , \quad (14)$$

and this is the dimensionless Poynting vector. When the sums (10) and (11) are substituted into Eq. (14), cross terms between all m values appear. The field lines of $\boldsymbol{\sigma}(\mathbf{r})$ are the flow lines of the radiated energy by the dipole.

5 Poynting vector and flow lines of energy

Let us first consider a dipole in free space, so we use only the $m = 0$ term above. We then find

$$\boldsymbol{\sigma}(\mathbf{r}) = \frac{\sin^2 \alpha}{q_0^2} \hat{\mathbf{r}}_0 , \quad (15)$$

with q_0 the dimensionless distance from the dipole to the field point, and $\hat{\mathbf{r}}_0$ is the radially outward unit vector from the dipole. Angle α is the angle between vector \mathbf{u} and the direction of observation, so $\cos\alpha = \hat{\mathbf{r}}_0 \cdot \mathbf{u}$. The Poynting vector $\boldsymbol{\sigma}(\mathbf{r})$ is proportional to $\hat{\mathbf{r}}_0$, and therefore the field lines are straight lines, coming out of the dipole. No radiation is emitted along the dipole axis ($\alpha = 0$). Figure 2 shows the field lines for a free dipole.

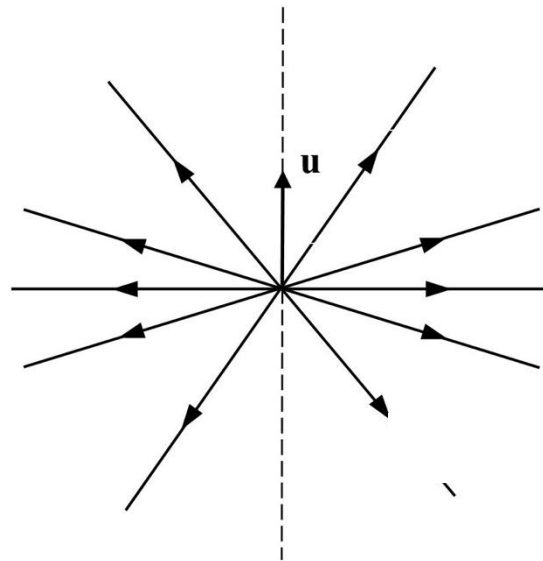


Fig. 2 The diagram shows the field lines of the Poynting vector for a free linear dipole. The dipole oscillates along the \mathbf{u} direction, and the field lines of energy flow are straight at all distances.

6. Energy flow lines between parallel mirrors

The field lines of the vector field $\boldsymbol{\sigma}(\mathbf{r})$ can be obtained numerically,¹⁴ and a typical example is shown in Fig. 3. The free parameters for the problem are the dimensionless distance $\ell = k_0 L$ between the mirrors, the dimensionless distance $h = k_0 H$ between the dipole and the lower mirror, and the angle γ between the dipole direction and the z axis. Shown are field lines in the $\bar{y}\bar{z}$ plane, with $\bar{y} = k_0 y$ to the right and $\bar{z} = k_0 z$ up. With $1/k_0$ as the length scale, 2π corresponds to an optical wavelength. In the figure we have $\ell = 4$, $\gamma = \pi/2$, and the dipole is located at the midway point between the mirrors. Close to the dipole, the electric and magnetic fields of the dipole diverge, so one may expect that in this region the field lines come straight out of the dipole, as for a free dipole. At larger distances, interference with the reflected field sets in, and close to the mirrors the field lines bend away from the mirrors, since radiation cannot penetrate the mirrors. Again, no radiation is emitted along the dipole axis, and we see from the figure that

field lines bend toward this axis, and end there. Fig. 4 shows the field lines for $\ell = 4$, $\gamma = \pi/2$, but now the dipole is closer to the bottom mirror. Below the dipole, field lines still come out of the dipole, but now they curve up and some return to the dipole at the other side. Above the dipole a singularity appears, which is indicated by a little circle. Apparently, close to the dipole the radiation from the dipole itself does not dominate the emission of radiation, since this would be emitted in the radially outward direction for all directions. Fig. 5 shows field lines for $\ell = 4$, $h=1$ and $\gamma = \pi/3$. The loop structure of Fig. 4 rotates with the dipole moment, and at the same time the field line structure becomes more intricate. Apparently, very close to the dipole the reflected field has a significant influence on the emission of radiation, except in the case of Fig. 3.

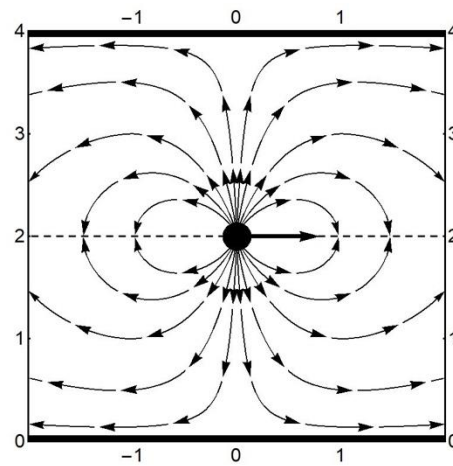


Fig. 3 Field line pattern for a horizontal dipole midway between the mirrors. The solid lines on top and bottom represent the mirrors.

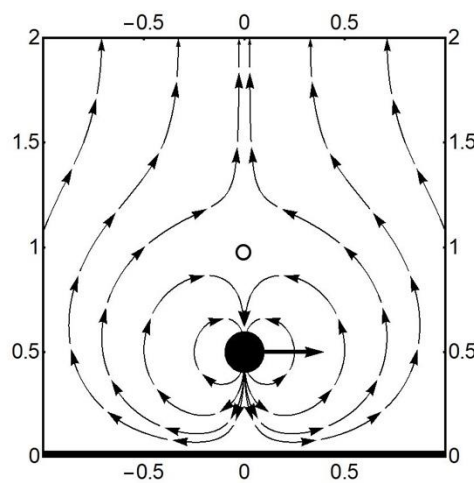


Fig.4 Field line pattern for a horizontal dipole, at a distance $h = 0.5$ from the bottom mirror. The top mirror at $\ell = 4$ is outside the picture.

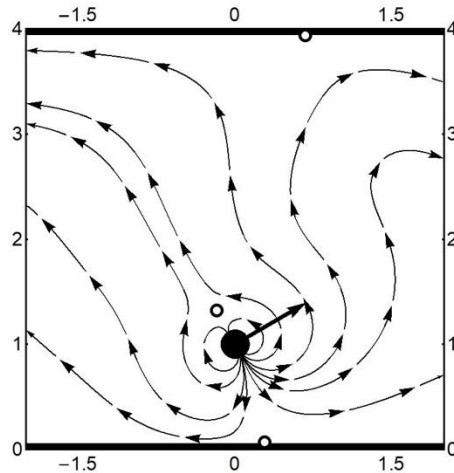


Fig.5 Field line pattern for $\ell = 4$, $h = 1$ and the dipole moment is tilted over 60° . Little circles indicate singular points of the flow field.

7. Emission of radiation

The electric and magnetic fields of the dipole itself are given by Eqs. 8 and 9 with $m = 0$. The distance to the dipole is q_0 . The electric field has terms with $1/q_0$, $1/q_0^2$ and $1/q_0^3$, and all these terms diverge for $q_0 \rightarrow 0$. Similarly, the magnetic field has terms with $1/q_0$ and $1/q_0^2$. Therefore, in Eq. (14) for the Poynting vector one would expect that the highest order term is $1/q_0^5$. We see from Eq. (15), however, that only the term with $1/q_0^2$ is present for a free dipole. All other combinations leading to terms with $1/q_0^3$, $1/q_0^4$ and $1/q_0^5$ cancel out exactly. The reflected electric and magnetic fields are finite at the location of the dipole. Therefore, in the Poynting vector we get a combination of the $1/q_0^3$ term of the electric field of the dipole with the reflected magnetic field. Such a term would give a $1/q_0^3$ contribution to the Poynting vector, and this would dominate the $1/q_0^2$ term of the radiation emitted by the free dipole. From Eq. 9 we can find the magnetic field of the images at the location of the dipole. We cross this with the $1/q_0^3$ term of the electric field of the dipole, giving the leading term in the Poynting vector in the neighborhood of the dipole. We obtain

$$\sigma(\mathbf{r}) = \frac{\sin \gamma}{q_0^3} \left[\mathbf{u}'(1 - 3\cos^2 \alpha) + 3\mathbf{u} \cos \alpha \cos \beta \right] \eta(h, \ell) + \dots \quad (16)$$

Vector \mathbf{u}' is defined as

$$\mathbf{u}' = \mathbf{e}_x \times \mathbf{u} \quad , \quad (17)$$

and angle α is defined above. Angle β is the angle between \mathbf{u}' and $\hat{\mathbf{r}}_0$ so $\cos \beta = \hat{\mathbf{r}}_0 \cdot \mathbf{u}'$. The dependence on h and ℓ is accounted for by the function and $\bar{z}_m = k_o z_m$. A typical example of the function $\eta(h, \ell)$ is given in Fig. 6.

$$\eta(h, \ell) = \sum_{m \neq 0} \frac{(-1)^m}{\alpha_m} \left(\cos \alpha_m - \frac{\sin \alpha_m}{\alpha_m} \right), \tag{18}$$

with

$$\alpha_m = \bar{z}_m - h, \tag{19}$$

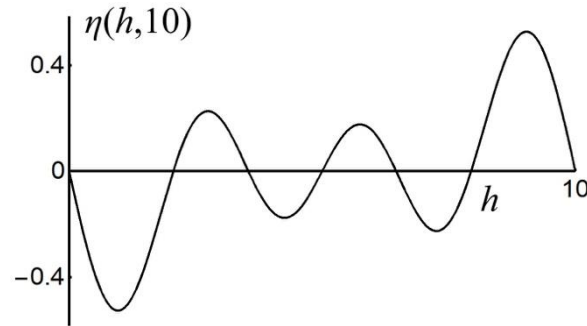


Fig.6 Shown is $\eta(h, \ell)$ as a function of h for $\ell = 10$.

To see the significance of the result shown in Eq. (16), we notice that the term of $\sigma(\mathbf{r})$ shown is in the $\bar{y}\bar{z}$ plane, since both \mathbf{u} and \mathbf{u}' are in the $\bar{y}\bar{z}$ plane. The dependence on the field point $(\bar{x}, \bar{y}, \bar{z})$ only comes in through the angles α and β . Vector \mathbf{u}' is perpendicular to the dipole direction vector \mathbf{u} . Let a field point be in the $\bar{y}\bar{z}$ plane on a line through the dipole and vector \mathbf{u}' . Then $\alpha = 90^\circ$, and so $\sigma(\mathbf{r})$ is into the direction of \mathbf{u}' for $\eta(h, \ell)$ positive. If a field point is in the $\bar{y}\bar{z}$ plane on a line through the dipole and vector \mathbf{u} , then $\beta = 90^\circ$, $\cos \alpha = \pm 1$, and $\sigma(\mathbf{r})$ is in the direction of $-2\mathbf{u}$. On completing the picture we see that we get closed loops in the $\bar{y}\bar{z}$ plane, with field lines coming out of the dipole at one end and returning to the dipole at the other end. The orientation of the loops depends on the sign of $\eta(h, \ell)$. For the examples shown in Figures 4 and 5 we have $\eta(h, \ell) < 0$, and the orientation is as shown in the figures (field lines coming out at the bottom and returning on top).

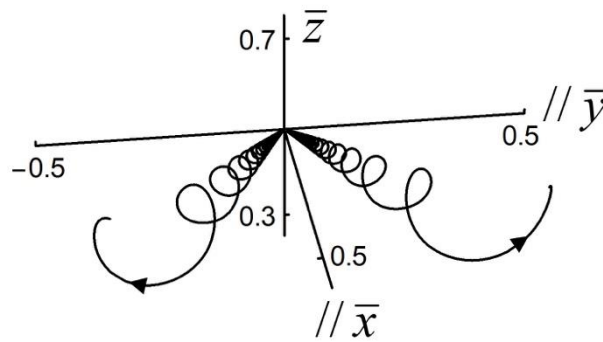


Fig. 7 Shown are spiraling field lines coming out of the dipole. The parameters are $\ell = 4$, $h = 0.5$ and $\gamma = \pi / 2$.

These parameters are the same as for the field line pattern in Figure 4. Behind the $\bar{y}\bar{z}$ plane are two more spirals that wind around the same singular lines. The \bar{x} and \bar{y} axes have been raised to the height of the dipole for clarity. Let us now consider field points off the $\bar{y}\bar{z}$ plane and close to the dipole. The higher order terms will give a radially outgoing component, so a field line will have the tendency to move away from the $\bar{y}\bar{z}$ plane, while the contribution from Eq. (16) is still in the $\bar{y}\bar{z}$ plane. This gives spiraling field lines, as illustrated in Figure 7. We see from the figure that the spirals appear to wind around singular lines. On a singular line, the Poynting vector vanishes, and it is easy to see that the term shown in Eq. (16) is zero for

$$\cos \alpha = \pm \frac{1}{\sqrt{3}} \quad , \quad \cos \beta = 0 \quad . \quad (20)$$

Equations (20) define a set of two lines. From $\cos \beta = 0$ it follows that the lines lie in a plane perpendicular to vector \mathbf{u}' , so the plane is spanned by \mathbf{u} and \mathbf{e}_x . In this plane, α is the angle between \mathbf{u} and a line. This gives two solutions: $\alpha = 54.7^\circ$ and $\alpha = 125.3^\circ$. These lines are indicated by ℓ_+ and ℓ_- in Fig. 8, and the direction of rotation of the Poynting vector around these lines is shown for $\eta(h, \ell) > 0$. The lines extend at the other side of the dipole (behind the $\bar{y}\bar{z}$ plane), and there the field lines also wind around these singular lines. A set of field lines forms a vortex structure, and so we conclude that radiation is emitted in a pattern of four vortices, provided that $\eta(h, \ell)$ is not exactly zero. The direction of rotation of the field lines around the singular lines is determined by the sign of $\eta(h, \ell)$. Another example of the vortex emission is shown in Fig. 9.

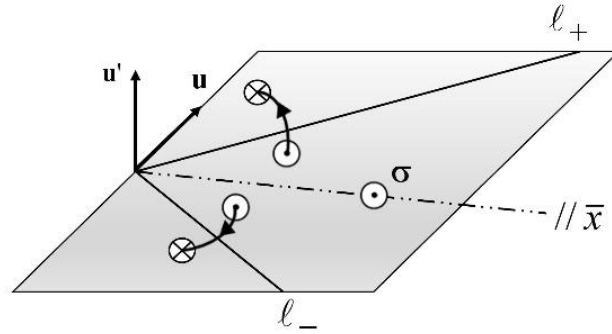


Fig.8 The figure shows the orientation of two singular lines, l_+ and l_- , which are singular lines at the centers of two vortices. The lines extend to the left, and these are center lines of two other vortices. The direction of rotation of the Poynting vector around these lines is illustrated for $\eta(h, \ell) > 0$.

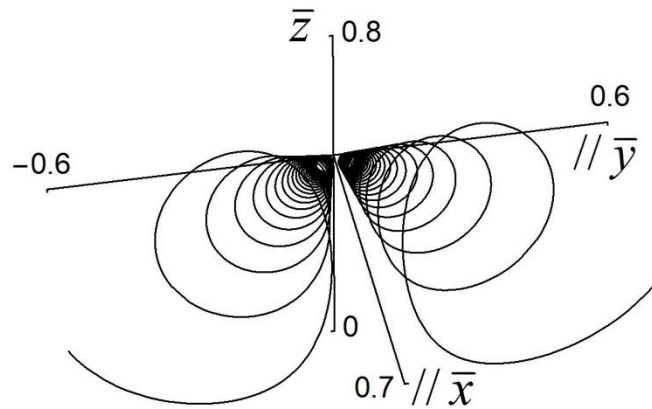


Fig. 9 Shown are two emission vortices for $\ell = 5.5$, $h = 0.5$ and $\gamma = \pi/2$.

8. The function $\eta(h, \ell)$

The strength of the vortices is proportional to function $\eta(h, \ell)$, and this function represents the dependence on h and ℓ of the Poynting vector close to the dipole. If this function is zero for certain values of h and ℓ , then the four vortices are absent. The spatial extent of the loops in the $\bar{y}\bar{z}$ plane and the vortices off the $\bar{y}\bar{z}$ plane are determined by the value of $\eta(h, \ell)$ for a given h and ℓ . We now look at this function in more detail. Combination of Eqs. (2) and (19) gives

$$\alpha_m = m\ell + (1 - (-1)^m)(\frac{1}{2}\ell - h) \quad , \quad (21)$$

or when split in odd and even

$$\alpha_m = \begin{cases} m\ell, & m \text{ even} \\ (m+1)\ell - 2h, & m \text{ odd} \end{cases} \quad . \quad (22)$$

For m even, we have $\alpha_{-m} = -\alpha_m$, and we see that the terms with m even in Eq.(18) cancel in pairs.

We get

$$\eta(h, \ell) = \sum_{m \text{ odd}} \frac{1}{\alpha_m} \left(\frac{\sin \alpha_m}{\alpha_m} - \cos \alpha_m \right) . \tag{23}$$

In order to evaluate the sum in Eq. (23), we notice the following integral representation

$$\eta(h, \ell) = \sum_{m \text{ odd}} \int_0^1 du u \sin(\alpha_m u) , \tag{24}$$

as can be checked by inspection. With α_m for m odd given in Eq. (22), this can also be written as

$$\eta(h, \ell) = \text{Im} \int_0^1 du u e^{-2ihu} \sum_{m \text{ odd}} e^{i(m+1)\ell u} , \tag{25}$$

and with Poisson's summation formula for the sum over m we obtain

$$\eta(h, \ell) = \frac{\pi}{\ell} \text{Im} \int_0^1 du u e^{-2ihu} \sum_{n=-\infty}^{\infty} \delta(u - \frac{n\pi}{\ell}) . \tag{26}$$

Integration over u then yields the alternative representation

$$\eta(h, \ell) = -\frac{\pi^2}{\ell^2} \sum_{n=1}^{[\ell/\pi]} n \sin\left(\frac{2n\pi h}{\ell}\right) , \tag{27}$$

where the upper limit $[\ell/\pi]$ is the integer part of ℓ/π . This new representation is a finite sum, as compared to the infinite series in representation (18).

The sum over m in Eq. (18) gives numerical convergence problems for small values of ℓ . The reason is obvious from Eq. (27): For $\ell < \pi$ the sum is empty, so we have

$$\eta(h, \ell) = 0, \quad \ell < \pi . \tag{28}$$

Since 2π corresponds to an optical wavelength, we conclude that the four-vortex structure is not present if the separation between the mirrors is less than half a wavelength. For $h=0$ and $h=\ell$ the sine functions in Eq. (27) are zero, so we have

$$\eta(0, \ell) = \eta(\ell, \ell) = 0 , \tag{29}$$

e.g., the function is zero at the endpoints (at the mirrors). At the midpoint between the mirrors we have $h = \ell/2$, which gives

$$\eta(\frac{1}{2}\ell, \ell) = 0 . \tag{30}$$

So there are no vortices if the dipole is at the midway point, as in Figure 3. It also follows from Eq. (27) that

$$\eta(\ell - h, \ell) = -\eta(h, \ell) \quad , \quad (31)$$

so the function is antisymmetric around the midpoint. The sine functions in Eq. (27) give oscillations as a function of h , as seen in Figure 6. At $h = \ell$ we have in the n -th term $\sin(2n\pi h / \ell) = \sin(2n\pi)$, and this corresponds to n full swings of the sine curve when at the top mirror. The largest value of n is $[\ell / \pi]$, and therefore the function $\eta(h, \ell)$ makes n full swings ($2n$ loops) on the range $0 \leq h \leq \ell$. Figure 10 shows $\eta(h, \ell)$ for $\ell = 40$, so $[\ell / \pi] = 12$, and we see indeed 12 swings in the figure.

Interestingly, the finite sum in Eq. (27) can be evaluated in closed form. We find

$$\eta(h, \ell) = \frac{\pi^2}{4\ell^2 \sin^2 x} \{2(N + 1) \sin x \cos[(2N + 1)x] - \sin[2(N + 1)x]\} \quad , \quad (32)$$

with $N = [\ell / \pi]$ and $x = \pi h / \ell$.

Finally, we mention that the limit of a single mirror can be found easily. When we set $\ell \rightarrow \infty$ for h fixed, we have $\alpha_m \rightarrow \infty$, except for $m = -1$. With $\alpha_{-1} = -2h$ we find from Eq. (18)

$$\eta(h, \infty) = \frac{1}{2h} \left[\cos(2h) - \frac{\sin(2h)}{2h} \right] \quad , \quad (33)$$

in agreement with earlier results.¹⁵

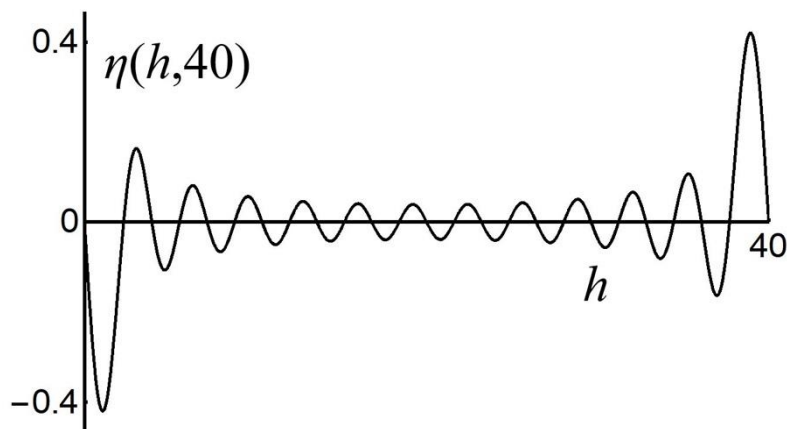


Fig. 10 The figure shows $\eta(h, 40)$, illustrating that the number of full swings is $[\ell / \pi]$, which is 12 here.

9. Conclusions

Electric dipole radiation in between parallel mirrors is emitted as four vortices, two of which are shown in Figs 7 and 9. This is a result of the interference between the directly emitted electric field by the dipole and the reflected magnetic field by the mirrors. Equation (16) gives the Poynting vector at very close distances to the dipole, and it is shown that this leading term is

responsible for the loops in Figs 4 and 5 and the vortices in Figs 7 and 9. The extent of the vortices is determined by the function $\eta(h, \ell)$, which only depends on the separation of the mirrors and the distance of the dipole to the lower mirror.

References

1. Morawitz, H. (1969): Self-coupling of a two-level system by a mirror. *Phys. Rev.*, 187; 1792-1796.
2. Drexhage, K. H. (1974): Interaction of light with monomolecular dye layers. *Prog. Opt.*, 12; 163-232.
3. Lukosz, W.; Kunz, R. E. (1977): Fluorescence lifetime of magnetic and electric dipoles near a dielectric interface. *Opt. Commun.*, 20; 195-199.
4. Lukosz, W.; Kunz, R. E. (1977): Light emission by magnetic and electric dipoles close to a plane interface. I. Total radiated power. *J. Opt. Soc. Am.*, 67; 1607-1615.
5. Chance, R. R.; Prock, A.; Silbey, R. (1978): Molecular fluorescence and energy transfer near interfaces. *Adv. Chem. Phys.*, 39; 1-65.
6. Sipe, J. E. (1981): The dipole antenna problem in surface physics: a new approach. *Surf. Sci.*, 105; 489-504.
7. Ford, G. W.; Weber, W. H. (1984): Electromagnetic interactions of molecules with metal surfaces. *Phys. Rep.*, 113; 195-287.
8. Novotny, L. J. (1997): Allowed and forbidden light in near-field optics. I. A single dipolar light source. *Opt. Soc. Am. A*, 14; 91-104.
9. Nha, H.; Jhe, W. (1996): Cavity quantum electrodynamics between parallel dielectric surfaces. *Phys. Rev. A*, 54; 3505-3513.
10. Philpott, M. R. (1973): Fluorescence from molecules between mirrors. *Chem. Phys. Lett.*, 19; 435-439.
11. Milonni, P. W.; Knight, P. L. (1973): Spontaneous emission between mirrors. *Opt. Commun.*, 9; 119-122.
12. Chance, R. R.; Prock, A.; Silbey, R. J. (1975): Decay of an emitting dipole between two parallel mirrors. *Chem. Phys.*, 62; 771-772.
13. Hulet, R. G.; Hilfer, E. S.; Kleppner, D. (1985): Inhibited spontaneous emission by a Rydberg atom. *Phys. Rev. Lett.*, 55; 2137-2140.
14. Xu, Z.; Arnoldus, H. F. (2017): Energy flow of electric dipole radiation in between parallel mirrors. *J. Mod. Opt.*, 64; 2123-2132.
15. Li, X.; Arnoldus, H. F. (2010): Electric dipole radiation near a mirror. *Phys. Rev. A*, 81; 053844-1-053844-10.